AD_____

Award Number: W81XWH-07-1-0601

TITLE: Early Diagnosis, Treatment and Care of Cancer Patients

PRINCIPAL INVESTIGATOR: Richard Fisher, M.D.

CONTRACTING ORGANIZATION: University of Rochester School of Medicine
Rochester, NY 14642

REPORT DATE: September 2012

TYPE OF REPORT: Final

PREPARED FOR: U.S. Army Medical Research and Materiel Command
Fort Detrick, Maryland 21702-5012

DISTRIBUTION STATEMENT: Approved for Public Release;
Distribution Unlimited

REPORT DOCUMENTATION PAGE

Form Approved
OMB No. 0704-0188

1. REPORT DATE	2. REPORT TYPE	3. DATES COVERED
September 2012	Final	1 September 2007 – 31 August 2012

4. TITLE AND SUBTITLE

Early Diagnosis, Treatment and Care of Cancer Patients

5a. CONTRACT NUMBER

5b. GRANT NUMBER
W81XWH-07-1-0601

5c. PROGRAM ELEMENT NUMBER

6. AUTHOR(S)

Craig T. Jordan
Richard I. Fisher

E-Mail: richard_fisher@urmc.rochester.edu

5d. PROJECT NUMBER

5e. TASK NUMBER

5f. WORK UNIT NUMBER

7. PERFORMING ORGANIZATION NAME(S) AND ADDRESS(ES)

University of Rochester School of Medicine
Rochester, NY 14642

8. PERFORMING ORGANIZATION REPORT NUMBER

9. SPONSORING / MONITORING AGENCY NAME(S) AND ADDRESS(ES)
U.S. Army Medical Research and Materiel Command
Fort Detrick, Maryland 21702-5012

10. SPONSOR/MONITOR'S ACRONYM(S)

11. SPONSOR/MONITOR'S REPORT NUMBER(S)

12. DISTRIBUTION / AVAILABILITY STATEMENT
Approved for Public Release; Distribution Unlimited

13. SUPPLEMENTARY NOTES

14. ABSTRACT

This grant program encompasses two complimentary projects. The hypothesis that leukemia can be treated effectively by inhibition of putative cancer stem cells will be tested in project #1. This will be done by application of inhibitors of stem cells as a novel approach for eradication of leukemia tumor cells. Parthenolide (PTL)-based drugs and related drugs that inhibit nuclear factor kappa B (NF-κB) will be used. The effects of these drugs will also be tested on normal hematopoietic cells. In project 2, studies will investigate how standard therapies effect normal CNS stem cells, and will attempt to develop less toxic regimens for the treatment of brain cancers. To this end, studies will determine whether parthenolide or related drugs cause CNS damage in animals treated with these substances, and will assess whether parthenolide can function as a chemosensitizing agent for various conventional chemotherapy drugs.

15. SUBJECT TERMS
leukemia, stem cell, cancer, parthenolide, oligodendrocyte, progenitor

16. SECURITY CLASSIFICATION OF:			17. LIMITATION OF ABSTRACT	18. NUMBER OF PAGES	19a. NAME OF RESPONSIBLE PERSON
a. REPORT	b. ABSTRACT	c. THIS PAGE			USAMRMC
U	U	U	UU	25	19b. TELEPHONE NUMBER *(include area code)*

Table of Contents

	Page
Introduction	**4**
Body	**4 – 17 Project 1**
	22 - 24 Project 2
Key Research Accomplishments	**18 Project 1**
	25 Project 2
Reportable Outcomes	**18 Project 1**
	25 Project 2
Conclusion	**18 Project 1**
	25 Project 2
References	**18-21 Project 1**
	N/A Project 2
Appendices	**N/A**

Introduction

This grant is comprised of two complementary projects. For the purposes of this report, progress for each project will be described separately below.

Body

Project 1

The objective of this project is to develop a novel therapeutic agent that specifically targets human leukemia stem cells (LSC). While the concept of a critical leukemia stem cell in myeloid disease has been postulated for over three decades, to date no therapeutic agent has been identified that specifically and preferentially ablates LSC in vivo. Thus, the central premise of this grant is that direct targeting of LSC will yield more effective therapy for leukemia. Previously, we demonstrated that parthenolide (PTL) is highly cytotoxic to LSC in vitro, but does not significantly affect normal hematopoietic stem cells (HSC). However, solubility of PTL is limiting; thus we have generated a PTL analog, dimethyl amino parthenolide (DMAPT), that is much more soluble in water and retains the anti-leukemic activity of PTL. Using this agent, the tasks below were specified:

SOW task #1: To demonstrate that a parthenolide analog can be used for preclinical and clinical applications related to treatment of chronic leukemia (Months 1-36).

Studies completed, please see progress reports from years 1-3.

SOW task #2: To demonstrate that a parthenolide analog can function as a chemosensitizing agent to enhance ablation of chronic leukemia cells (Months 37-60).

In order to identify optimal drug combinations to employ with parthenolide, we have performed a series of studies designed to determine the central molecular properties of parthenolide. Our rationale has been that if we can understand the specific pathways modulated by parthenolide, then we can make rational predictions regarding how to use this compound in combination with conventional agents to achieve chemosensitization. In the following sections we provide a detailed analysis and summary of drug mechanism:

Primitive primary human AML cells differentially express genes required for control of redox state

Extensive previous studies have demonstrated that more primitive hematopoietic stem and progenitor cells reside within a small subset of bone marrow cells expressing the CD34

surface antigen (23). In addition, it has been demonstrated that primitive AML cells also generally express CD34 and are more resistant to conventional chemotherapy (20-22). Thus, in order to focus our studies specifically on the most critical subpopulations, we isolated CD34+ cells from AML patients (Supplemental Table 1) and normal bone marrow (NBM) donors for studies presented in this manuscript.

To investigate differences in the antioxidant machinery of primary AML vs. normal hematopoietic cells, we compared protein expression of all major antioxidant genes. Because recent studies have demonstrated many conventionally used "house-keeping" genes are differentially expressed in cancer vs. normal tissues (24, 25), and we consistently found GAPDH protein level differs significantly in CD34+ AML vs. CD34+ NBM cells (Supplemental Figure 1), we chose to compare protein expression of antioxidant genes from the same number of cells (Figure 1B) or the same amount of protein lysates (Supplemental Figure 2). As shown in Figure 1B, probing the lysates from equal numbers of CD34+ AML (n=9) and NBM cells (n=4) revealed comparable levels of SOD1 protein expression. However, SOD2 and CAT protein expression appeared to be down-regulated in about half of AML specimens examined, suggesting SOD and/or CAT functions are compromised in some AML specimens. In contrast, we found that the majority of AML specimens had up-regulated protein expression of glutathione pathway components including GCLC, GCLM, and GSS, which are required for glutathione biosynthesis, and GPX1 and GSR, which are involved in glutathione homeostasis. In addition, GSTP1 protein which is known to be over-expressed in several hematopoietic malignances including childhood acute lymphoblastic leukemia (26) and chronic lymphoblastic leukemia (27) was also up-regulated in our cohort of primary AML specimens. Lastly, TXN protein was up-regulated in a majority of AML patients as well. To exclude the possibility that the differences described above were due to a higher protein yield in leukemic vs. normal specimens, we also compared the expression of these anti-oxidant genes within equal amounts of total protein from each specimen (Supplemental Figure 2). The results consistently demonstrated a global up-regulation of glutathione pathway components in CD34+ AML specimens.

To gain further insight on the differential expression of redox genes, we compared their mRNA expression as well. We used mean expression of *HPRT1*, *GUSB*, and *TBP* as reference to internally normalize the expression of each gene within each specimen (Supplemental Figure 3A, B, C, D). Average expression of each gene in CD34+ NBM (n=4) cells was set to 1, and the relative expression of each gene in each specimen was calculated accordingly. Shown in Figure 1C, in 9 out of 10 genes examined (except for GCLM), mRNA levels between AML and NBM cells mirrored the direction of differences we observed at the protein level. For example, CD34+ AML cells have significantly down-regulated expression of *SOD2* (0.16 fold, p=0.046), and up-regulated expression of *GSS* (1.22 fold, p=0.041), *GPX1* (3.42 fold, p=0.016) and *TXN* (1.27 fold, p=0.041) mRNA (Figure 1C, also see Supplemental Figure 3E), consistent with the differences we observed in our western blot analysis (Figure 1B). For many genes the degree of difference at the protein level surpasses the differences in mRNA expression, suggesting redox genes may be regulated at both the transcriptional and translational level. Importantly, of the 6 genes directly involved in glutathione biosynthesis and homeostasis (*GCLC, GCLM, GSS, GPX1, GSR* and *GSTP1*), 5 had elevated mRNA and protein expression in the AML specimens, indicating a global up-regulation of the glutathione pathway in CD34+ primary AML cells.

Primary human AML cells have aberrant glutathione metabolism

To directly compare glutathione pathway activity in primary human AML and normal cells, we quantified the amount of reduced (GSH) and oxidized (GSSG) glutathione in isolated CD34+ NBM (n=4) and CD34+ AML (n=11) cells. Our results show that, compared to CD34+ NBM cells, GSH level is significantly lower and GSSG level is generally higher in CD34+ AML cells (Figure 2A, B). As a result, CD34+ AML cells have significantly less total glutathione (sum of GSH and GSSG) as well as a significantly decreased GSH to GSSG ratio (Figure 2C, D). These data indicate an aberrant glutathione homeostasis in CD34+ primary AML cells.

We next compared glutathione turnover rate in CD34+ AML and CD34+ NBM cells. CD34+ AML and NBM cells were isolated and cultured in media with isotope-labeled cystine ($^{13}C^{15}N$-Cystine). We measured newly synthesized glutathione ($^{13}C^{15}N$-glutathione) as percentage of total glutathione over time in each cell type. Over half of the AML specimens tested had a greater glutathione turnover at all time points compared to CD34+ NBM specimens (Figure 2E, F). In particular, after 8 hours, the percentage of newly synthesized glutathione is significantly higher in CD34+ AML cells comparing to CD34+ NBM cells (Figure 2G). These data indicate glutathione turnover rate is higher in AML specimens, suggesting glutathione synthesis and consumption are elevated in AML cells.

Primitive human AML cells are differentially sensitive to agents that deplete glutathione

The aberrant glutathione metabolism documented in Figure 2 suggests that AML cells might be vulnerable to further inhibition of glutathione pathway activity. Consequently, we investigated the activity of several experimental agents that are predicted to modulate glutathione metabolism. We first studied parthenolide (PTL), which we have previously shown is toxic to primary AML cells (including leukemic stem and progenitor populations) while sparing normal cells (19). PTL contains an active alpha, beta-unsaturated-gamma-lactone group (Figure 3B, red circular area) that should readily react with the free thiol group of glutathione. Indeed, PTL induced a dose-dependent decrease of cellular glutathione within 2 hours of treatment in AML cells (n=3, Figure 3A). We then compared CD34+ cells from AML patients (n=5) and NBM donors (n=5) treated with 7.5uM PTL to determine the change of total glutathione as a function of time. All CD34+ AML specimens experienced >95% of maximal glutathione depletion after 4 hours of PTL treatment (red lines, Figure 3B). However, normal CD34+ cells treated with a same dose of PTL responded with only 60-80% maximal glutathione depletion at 4 hours, followed by a robust rebound of cellular glutathione (up to 100% of untreated state) between 4-10 hours (black lines, Figure 3B). These data indicate glutathione homeostasis in AML cells is more vulnerable to PTL treatment. Importantly, this vulnerability correlates directly with cytotoxicity. Consistent with our previous findings, 7.5uM PTL treatment induced significantly more cell death in CD34+ AML cells than CD34+ NBM cells (Figure 3C). Taken together, these results suggest aberrant glutathione metabolism in AML cells can be targeted to induce AML-specific cell death.

Severe and sustained depletion of the cellular glutathione pool is known to induce oxidative stress and stimulate apoptosis (28-30). We observed the induction of anti-oxidant defenses such as heme oxygenase 1 (HO-1) at 4 hours following PTL treatment (Figure 3D), the point at which glutathione depletion reaches maximal (Figure 3B). Onset of apoptosis

pathway activity as indicated by cleavage of caspase 3 and PARP began at 4 hours, and maximized at 6 hours (Figure 3D). Importantly, PTL-induced reduction of glutathione clearly occurs before the onset of apoptosis (Figure 3B), indicating that glutathione loss precedes apoptosis and is not a non-specific downstream consequence of apoptotic mechanisms.

To expand our studies beyond PTL, we also investigated piperlongumine (PLM), a compound with a potentially similar mechanism-of-action. PLM was selected for two reasons: 1) It contains two functional alkene (olefin) groups that are adjacent to each of its ketone groups, indicating that PLM should be a potent electrophile, with a chemical structure similar to PTL (31) (red circular areas, Figure 3E). 2) A recent study reported PLM displays selective toxicity towards many types of cancer cells, an activity associated with induction of ROS (32).

We first confirmed the ability of PLM to deplete cellular glutathione in a dose-dependent manner (Supplemental Figure 4). At a 10uM dose, PLM achieved a very similar degree of glutathione depletion as PTL at 7.5uM. Consequently, we treated CD34+ AML (n=3) and CD34+ NBM cells (n=2) with 10uM PLM and monitored the change of cellular glutathione over time. Similar to the activity of PTL, we observed that a 4 hour treatment with PLM induced a >90% maximal glutathione depletion in leukemic cells, but only ~60% maximal glutathione depletion in CD34+ NBM cells (Figure 3E). Importantly, consistent with its selective toxicity to many other cancer types (32), 24 hours treatment with 10uM PLM strongly induced cell death in CD34+ AML cells, but only limited toxicity in CD34+ NBM cells (Figure 3F). Lastly, while PLM treatment in CD34+ AML cells induces severe glutathione depletion as soon as 2 hours, PARP and caspase-3 cleavage were only evident at around 6 hours post PLM treatment (Supplemental Figure 4), again indicating that glutathione depletion precedes the onset of cell death.

Overall, these data suggest CD34+ primary AML cells are more sensitive to agents depleting glutathione. In addition, the differential response of CD34+ AML vs. NBM cells further indicate an intrinsic difference between mechanisms regulating the glutathione pathway in leukemic and normal cells.

Parthenolide directly binds to multiple glutathione pathway components

To further investigate how PTL affects cellular glutathione metabolism, we employed more detailed analyses using biochemical and genetic approaches. Reactive cysteine sites are known to be important for enzymatic function of many glutathione pathway components including GCLC, GCLM and GPX1 (33-38). Given the fact that agents like PTL contain active moieties that readily react with accessible cysteines containing free thiol groups, we reasoned that this class of agents should further inhibit glutathione pathway activities by directly binding to and interfering with enzymes that regulate this pathway. To test this premise, we employed a biotinylated analogue of PTL for biochemical studies. As we have previously described, PTL can be converted to the stereoisomer melampomagnolide B (MMB), as a first step in the chemical process of adding a biotin moiety (Figure 4A). Importantly, MMB-biotin retains the biological activity of PTL, albeit at a slightly reduced potency due to steric hindrance of the biotin moiety. Using MMB-biotin, we previously performed pull-down experiments and identified known binding partners of PTL, such as IKK-beta and the NF-kB p65 (39). Here we employed an analogous strategy to investigate interactions of PTL with regulators of the glutathione pathway. CD34+ primary human AML

cells were treated with MMB-biotin, lysed, and then incubated with streptavidin beads to purify all protein targets of PTL. Subsequent studies using liquid-phase-mass-spectrometry (LC-MS/MS) identified GCLC and GPX1 as direct binding targets of PTL along with antioxidant protein TXN (Figure 4C).

To test the specificity of binding events between PTL and its protein targets, we carried out a competitive binding assay. As outlined in Figure 4B, CD34+ primary AML cells were pretreated with or without PTL followed by MMB-biotin treatment. Lysates were made from each treatment group and then passed over a streptavidin column to enrich for proteins that are directly bound by MMB-biotin. This methodology allowed us to identify specific binding targets of PTL. Using this approach, we successfully pulled down GCLC, GCLM, GPX1, and TXN proteins from cells that were treated with MMB-biotin (Figure 4C, lane 5). Importantly, a pretreatment with PTL competed the binding of MMB-biotin to GCLC, GCLM, GPX1, and TXN, indicating that these interactions were specific (Figure 4C, lane 6). IKK-beta, a known binding target of PTL was used as a positive control for our assay (40).

To gain insights into these binding events at the molecular level and to predict their functional consequences, we built structures of the human GCLC/GCLM complex and GPX1 protein based on available crystal structures of their homologous proteins, and subsequently modeled docking events of PTL to accessible cysteines (Figure 4D, E). Our results show there are multiple cysteines in GCLC, GCLM, and GPX1 proteins that are available for PTL binding. In general, these binding events could result in protein instability or specific enzyme activity loss. For example, Cys 249 of GCLC is evolutionarily conserved and resides near the glutamate-binding site (34). Therefore, this binding event would potentially interfere with the enzymatic function of GCLC (Figure 4D, green box). In addition, PTL readily forms covalent bonds with Cys 553 of GCLC and Cys 193, 194 of GCLM (Figure 4D red box), which have been proposed to be involved in inter-subunit disulfide bond formation between GCLC and GCLM (35, 36). Formation of the GCLC and GCLM heterodimer is important for the holoenzyme activity of GCL (38), suggesting such binding events could disrupt GCL holoenzyme formation and consequently diminish its activity. In the case of GPX1, selenocysteine Se-Cys 49 is known as the active center of glutathione peroxidase (41). Therefore, binding between PTL and Se-Cys 49 of GPX1 could potentially impair GPX1 enzymatic function (Figure 4E).

Targeting glutathione pathway enzymes GCLC and GPX1 is important for the anti-leukemia activity of PTL

To further study the functional consequence of binding events between PTL and its targets, we measured the expression of proteins following PTL treatment. We found that GCLC protein level decreased in all primary AML specimens (n=3) as well as in the leukemic cell line M9-ENL cells (42) (Figure 5A). GPX1 protein level also decreased in most cases as well (Figure 5A). These data suggest degradation of GCLC and GPX1 is a component of PTL-mediated cell death in AML cells. If so, decreasing the function of these genes should render AML cells more sensitive to PTL. To test this hypothesis, we performed shRNA-mediated knock down of *GCLC* and *GPX1* mRNA expression in the M9-ENL cell line and tested their sensitivity to PTL treatment. Clone A of sh-GCLC achieved a very efficient reduction in *GCLC* mRNA and protein (Figure 5B, C), which resulted in a significantly increased sensitivity to PTL treatment (Figure 5D). Similarly, clone B of sh-GPX1 successfully

knocked down *GPX1* mRNA and protein expression (Figure 5E, F), resulting in increased sensitivity to PTL as well (Figure 5G). These data indicate GCLC and GPX1 degradation are functionally important to PTL toxicity. Notably, both GCLC and GPX1 expression are up-regulated in AML cells (Figure 1B, C), suggesting PTL-induced GCLC and GPX1 degradation could increase selective toxicity towards AML cells.

Cellular glutathione pathway activity determines parthenolide sensitivity in solid tumors

To extend our analysis beyond leukemic cell types, we correlated relative PTL sensitivity and global gene expression profile of 307 solid tumor cell lines (multiple histologies) to determine gene functions that are associated with PTL resistance (Supplemental Table 2). This study identified *GPX2*, a gastrointestinal glutathione peroxidase (presumably the solid tumor equivalent of *GPX1*), as the top ranked gene associated with PTL resistance. In addition, *GCLC* and *SLC7A11*, a subunit of the cystine transporter upstream of glutathione biosynthesis, were correlated with PTL resistance as well. These findings indicate cancer cells with elevated glutathione pathway activity will be more resistant to PTL. This is consistent with the results of *GCLC* and *GPX1* knock-down experiments showing AML cells with decreased GCLC and GPX1 function are more sensitive to PTL. Together, these studies indicate glutathione pathway activity is a critical determinant of PTL toxicity in AML cells, as well as other solid tumor types.

Parthenolide and piperlongumine represent a novel class of anti-leukemic agents

Our findings of aberrant glutathione metabolism in CD34+ primary AML cells as well the abilities of PTL-like agents in targeting the glutathione pathway raised the possibility that PTL-like agents may represent a fundamentally different type of drug relative to the agents typically employed for leukemia therapy. To investigate this issue in more detail, we first performed side-by-side efficacy test of PTL and PLM in comparison to the front line AML drug cytarabine (Ara-C) and the anthracycline idarubicin (IDA). Shown in Figure 6A and B, when 9 primary human AML specimens were treated with Ara-C or IDA, CD34+ populations in more than half of the specimens displayed a significant level of resistance (Figure 6A, B). This is presumably due to the fact that CD34+ AML cells are enriched for more quiescent stem and progenitor cells, and are relatively more resistant to chemotherapy (20-22). In contrast, 7.5uM PTL, which is well tolerated by CD34+ NBM cells, showed 75-95% toxicity to 7 out of 9 specimens tested (Figure 6C). We observed similar results when this group of AML cells was treated with PLM, where 10uM PLM induced 60-95% toxicity to 7 out of 9 specimens (Figure 6D). These findings are noteworthy in that conventional agents, like PTL/PLM, are also known to induce oxidative stress (9), however as clearly shown in Figure 6, they are markedly less active towards CD34+ AML cells. This observation prompted us to investigate the mechanisms controlling oxidative stress induction in more detail and to ask whether the differential toxicity of PTL/PLM is correlated to their ability to modulate glutathione pathway activities. To this end, we treated AML specimens with each drug and monitored the change of glutathione following treatment. As shown in Figure 6E, in striking contrast to PTL and PLM, treatment with Ara-C and IDA did not significantly change total glutathione level in CD34+ AML cells. This finding was also verified in the M9-ENL cell line. When M9-ENL cells were treated with each drug at doses that resulted in comparable cell death (Figure 6F), PTL and PLM induced dramatic glutathione depletion, but Ara-C and IDA had little to no effect on

cellular glutathione contents (Figure 6G). Together, these data clearly indicate PTL and PLM possess a unique ability to inhibit the cellular glutathione system and are effective against CD34+ primary human AML cells, thereby representing a class of anti-leukemic agents that function by a distinctly different mechanism-of-action in comparison to standard chemotherapy agents.

Toxicity of PTL in combination with conventional anti-leukemic agents cytarabine and idarubicin

Our findings of aberrant glutathione metabolism in CD34+ primary AML cells as well the abilities of PTL-like agents in targeting the glutathione pathway raised the possibility that combining PTL-like agents with conventional drugs might be a beneficial strategy. Thus, we tested whether combinations of such agents could act to synergistically induce AML cell death. Three primary AML specimens were treated with either Ara-C or IDA alone or in combination with PTL. The toxicity of each drug combination is presented in Figure 7A (PTL + Ara-C) and 7B (PTL + IDA). In all AML specimens tested, addition of PTL was beneficial in terms of overall cytotoxic activity. Notably, a modest dose of PTL (5uM) combined with a sub-optimal dose of Ara-C (5uM) or IDA (60nM) resulted in 82%-93% cell death in all specimens tested (red bars, Figure 7A, B). To better quantify the effect of PTL with Ara-C or IDA, we calculated the potential synergy of each drug combination, where the combination index score (CI) indicates synergism ($0.4 < CI < 0.6$), moderate synergism ($0.6 < CI < 0.8$), slight synergism ($0.8 < CI < 0.9$), additivity ($CI > 0.9$), or antagonism ($CI > 1.1$). The results of this analysis were converted into a heat map format to better illustrate the data (Figure 7C). We found that the PTL and Ara-C combination displayed strong to slight synergism in all three AML specimens tested, although a different dose combination was required to achieve maximum synergy for each AML. In the case of the PTL and IDA, the combination showed synergy in one specimen (CD34+ AML2), with additive effects in two additional specimens (CD34+ AML 7, and 8). Together these results suggest agents like PTL can be combined with conventional chemotherapy to target more resistant CD34+ primary AML cells.

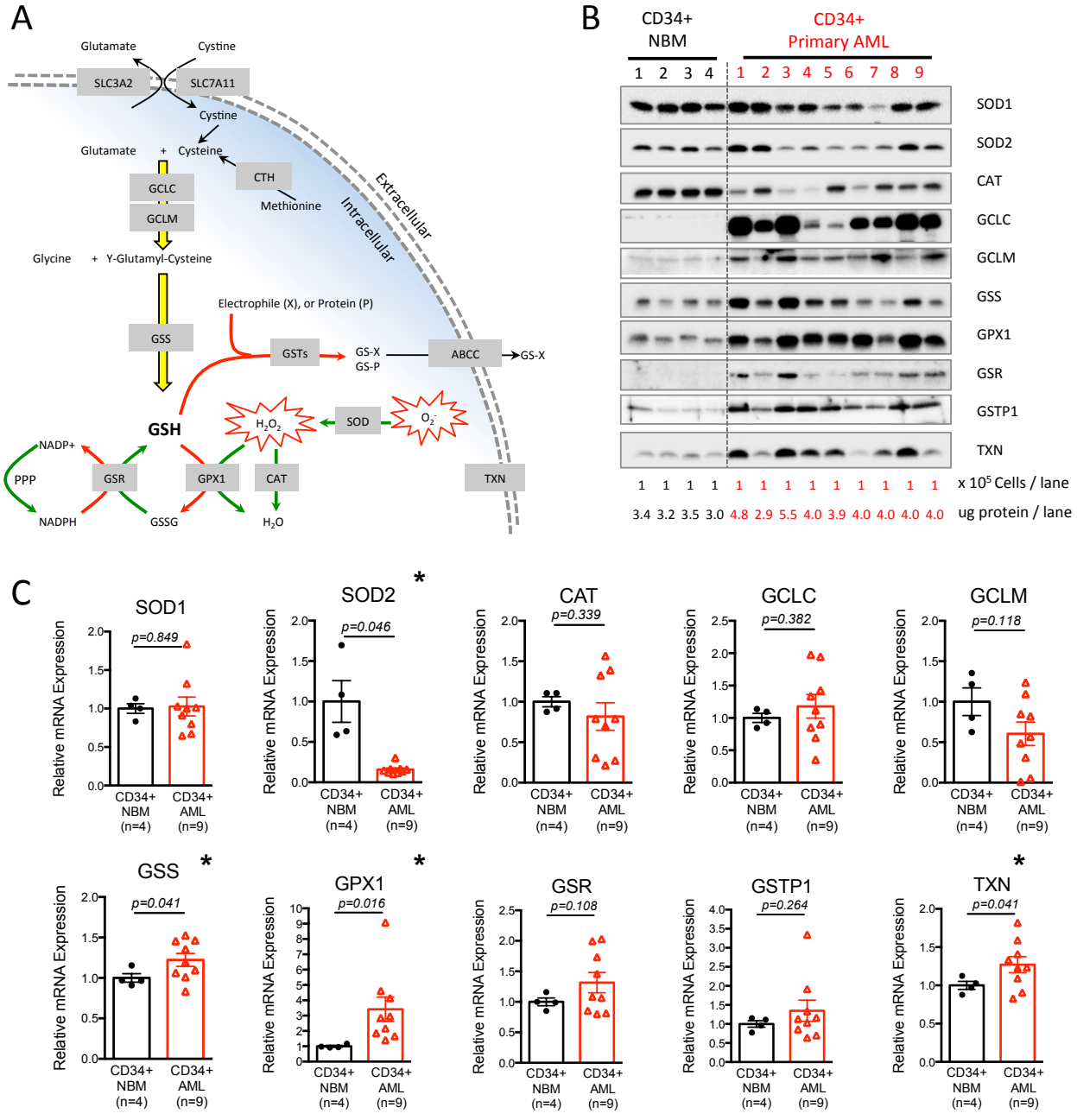

Figure 1

Primitive primary human AML cells differentially express genes required for control of redox state.
(A) Schematic diagram showing major antioxidant machineries required for control of redox state. **(B)** Expression of major antioxidant proteins in freshly isolated primary human CD34+ NBM (n=4) and CD34+ AML (n=9) specimens. Lysates from equal number of cells (100K) were loaded in each lane. Total amount of protein was quantified and presented as microgram (ug) protein per lane. **(C)** Relative mRNA expression of major antioxidant genes in freshly isolated primary human CD34+ NBM (n=4) and CD34+ AML (n=9) specimens. Mean expression of *HPRT1*, *GUSB*, and *TBP* was used as reference to internally normalize the expression of each gene within each specimen. Average expression of each gene in CD34+ NBM (n=4) cells was set to 1,

and the relative expression of each gene in each specimen was calculated accordingly and presented as dot plot. Mean ± SEM of each group is presented . * indicates a significant difference.

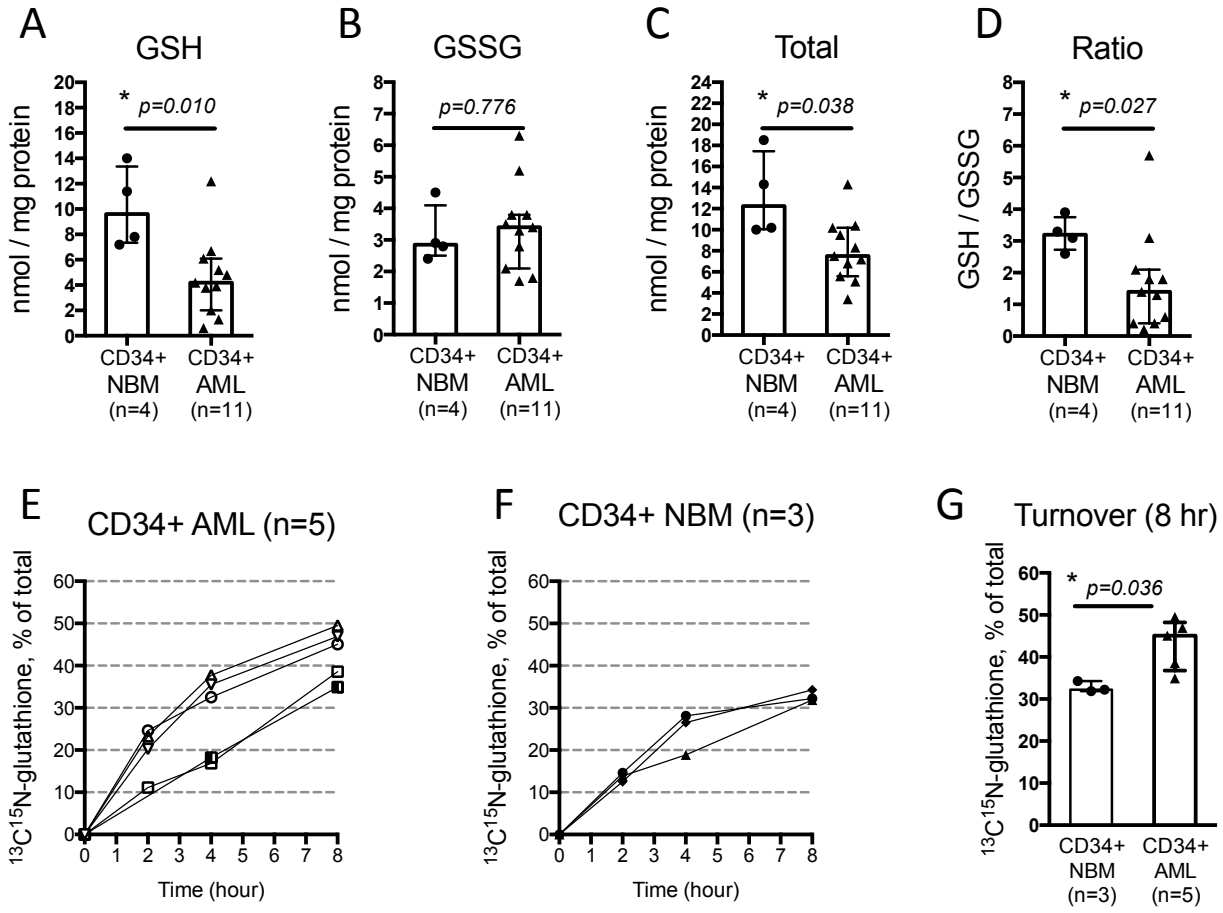

Figure 2

Primary human AML cells have aberrant glutathione metabolism.

Amount of reduced (GSH) **(A)**, oxidized (GSSG) **(B)**, total glutathione (sum of GSH+GSSG) **(C)**, and GSH to GSSG ratio **(D)** in each specimen. (**E, F**) Time-dependent increase of newly synthesized glutathione ($^{13}C^{15}N$-glutathione) as percentage of total glutathione in CD34+ NBM cells (n=3) and CD34+ AML cells (n=5). (**G**) Glutathione turnover at 8 hours post culturing CD34+ NBM (n=3) or CD34+ AML (n=5) cells in media with $^{13}C^{15}N$-labeled cystine. In A, B, C, D and G, each dot represents the value of each specimen. Median ± IQR (Inter-Quartile Range) of each group is presented as error bar. * indicates a significant difference.

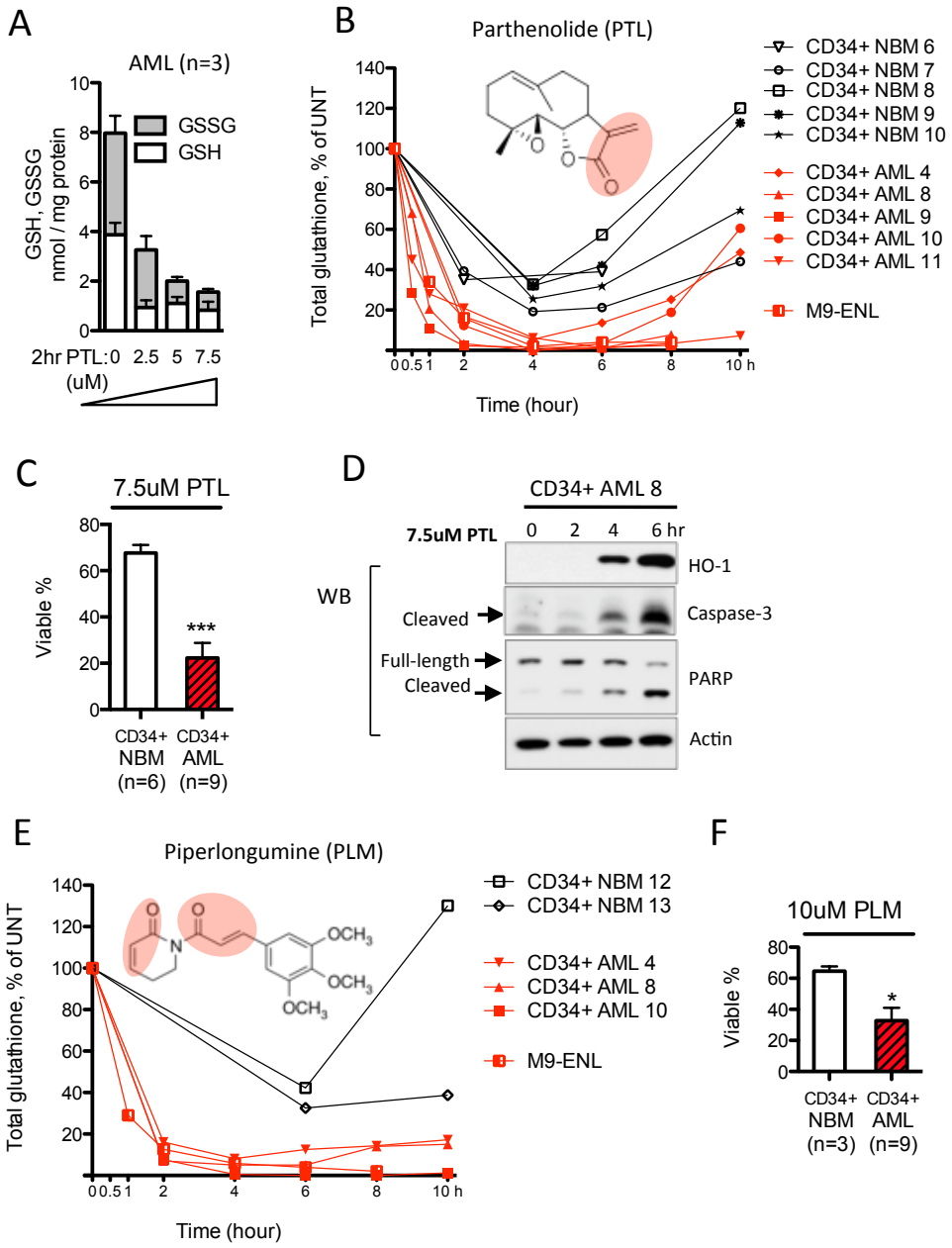

Figure 3

Primitive human AML cells are differentially sensitive to agents that deplete glutathione.
(**A**) PTL-induced dose-dependent glutathione depletion in primary human AML cells (n=3). (**B**) Structure of PTL and PTL-induced cellular glutathione level change as a function of time. Red lines indicate changes in CD34+ AML cells (n=5) and AML cell line M9-ENL cells. Black lines indicate changes in CD34+ NBM cells (n=5). (**C**) Percentage of viable cells after being cultured with 7.5uM PTL for 24 hours. (**D**) Western blot showing 7.5uM PTL induced protein expression change of oxidative stress and apoptosis markers. (**E**) Structure of PLM and PLM-induced cellular glutathione level change as a function of time. Red lines indicate changes in CD34+ AML cells (n=3) and AML cell line M9-ENL cells. Black lines indicate changes in CD34+ NBM cells (n=2). (**F**) Percentage of viable cells after being cultured with 10uM PLM for 24 hours. In C and F, Mean ± SD of each group is presented as bar graph. ***p<0.0005, *p<0.05.

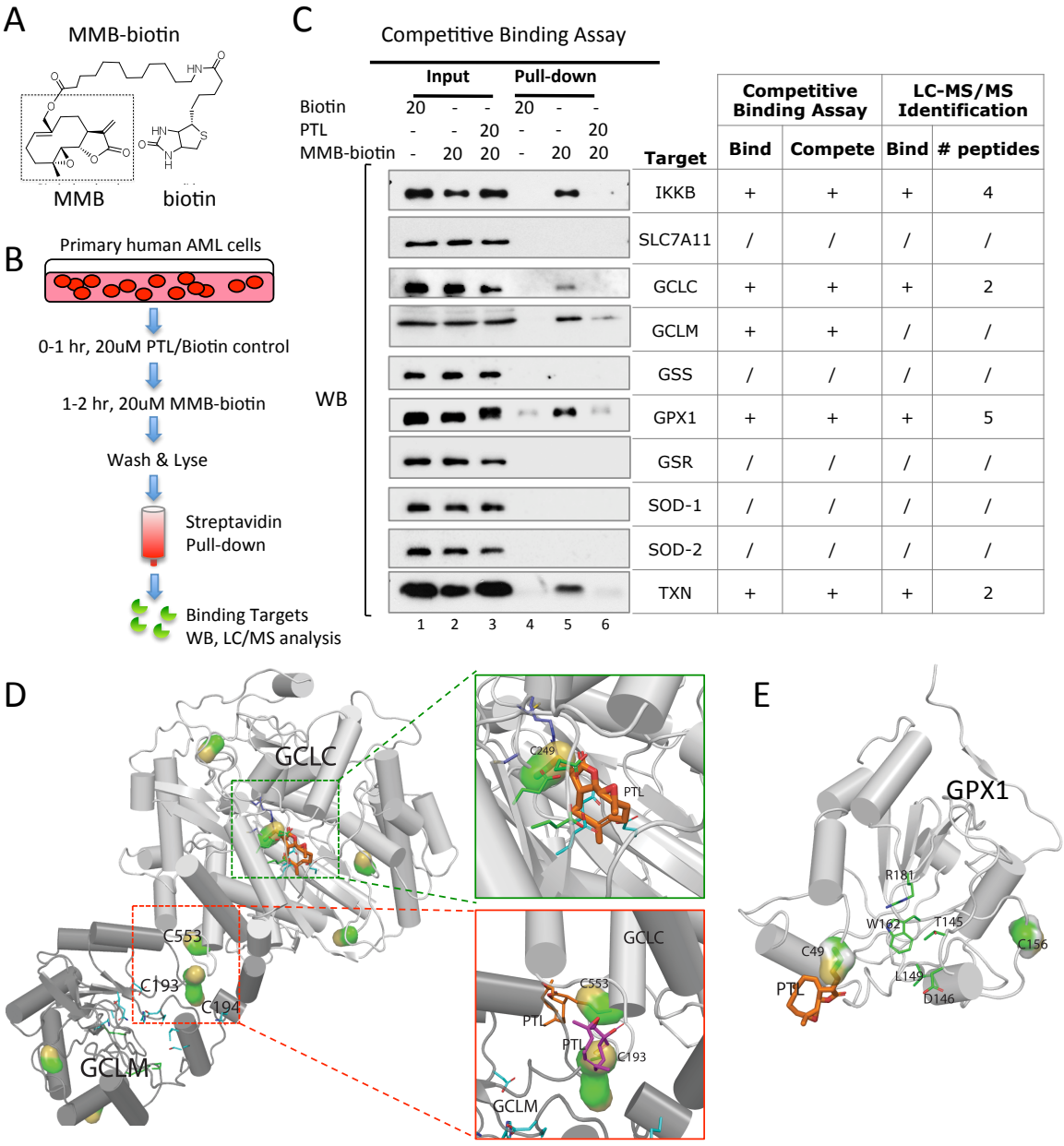

Target	Competitive Binding Assay		LC-MS/MS Identification	
	Bind	Compete	Bind	# peptides
IKKB	+	+	+	4
SLC7A11	/	/	/	/
GCLC	+	+	+	2
GCLM	+	+	/	/
GSS	/	/	/	/
GPX1	+	+	+	5
GSR	/	/	/	/
SOD-1	/	/	/	/
SOD-2	/	/	/	/
TXN	+	+	+	2

Figure 4

Parthenolide directly binds to multiple glutathione pathway components.

(**A**) Chemical structure of MMB-biotin. Dashed box outlines the part of molecule retains intact structure of MMB, a stereoisomer of PTL. (**B**) Schematic diagram showing the procedure of competitive binding assay. (**C**) Antioxidant proteins identified as PTL binding targets via competitive binding assay. Input and pull-down products from cell lysates of AML cells treated with biotin alone (lane 1, 4), MMB-biotin alone (lane 2, 5), or PTL followed by MMB-biotin (lane 3, 6) were probed with antibodies against various proteins. Pull-down products from MMB-biotin treated AML cell lysates were also subjected to LC-MS/MS analysis, and the results are presented side-by-side with competitive binding assay results in the table. "+" indicates a positive result, and "/" indicates a negative result. Numbers indicate number of peptides recognized by MS/MS for the identification any specific protein targets. (**D, E**) Covalent docking results of PTL to GCLC/GCLM holoenzyme complex (D) and GPX1 (E). The L-glutamate binding site of GCLC is enlarged in green box, and the heterodimer interface of GCLC/GCLM complex is in red box. The cysteines covalently attached with PTL are shown as surface representations, while the PTL structure is shown as thick sticks. Side chains of the key residues involved in enzymatic functions are shown as thin sticks.

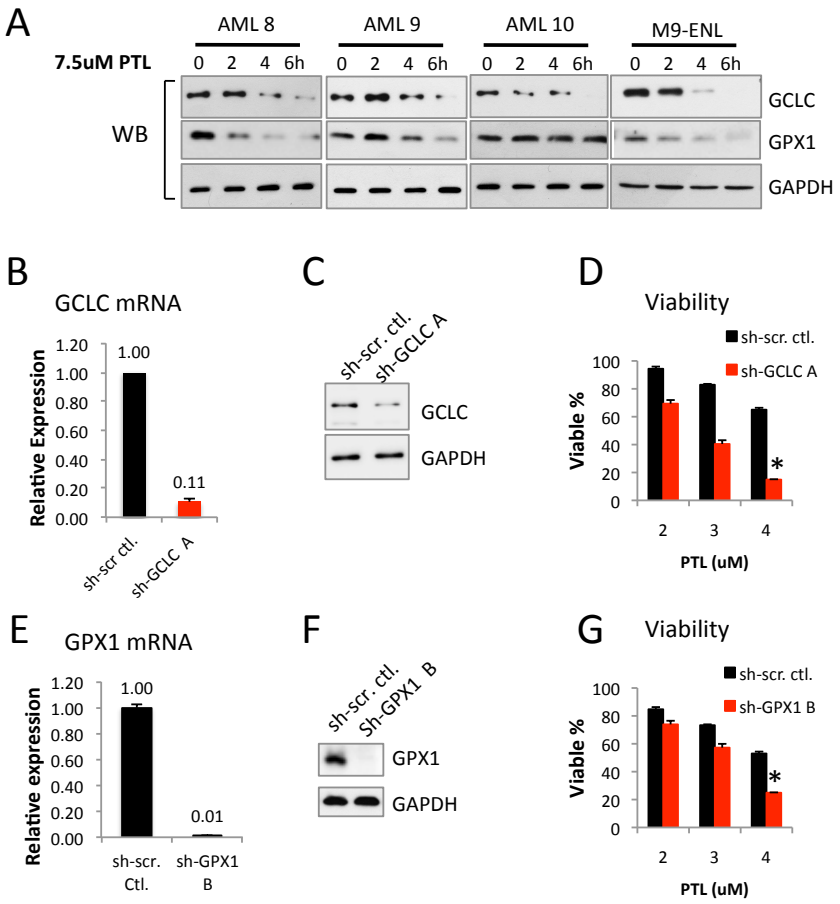

Figure 5

Targeting glutathione pathway enzymes GCLC and GPX1 is important for the anti-leukemia activity of PTL.

(**A**) Western blot showing 0, 2, 4, 6 hour GCLC and GPX1 protein expression in primary human AML cells (n=3) and M9-ENL cells treated with 7.5uM PTL. GAPDH is probed as loading control. Expression of *GCLC* mRNA (**B**) and protein (**C**) in M9-ENL cells infected with scramble shRNA control (sh-scr ctl.) or shRNA targeting *GCLC* (sh-GCLC A). (**D**) Percentage of viable M9-ENL cells after being cultured with increasing doses of PTL for 24 hours. Expression of *GPX1* mRNA (**E**) and protein (**F**) in cells infected with scramble shRNA control (sh-scr ctl.) or shRNA targeting *GPX1* (sh-GPX1 B). (**G**) Percentage of M9-ENL cells after being cultured with increasing doses of PTL for 24 hours. Error bars represent mean ± SD of triplicates. *p<0.05.

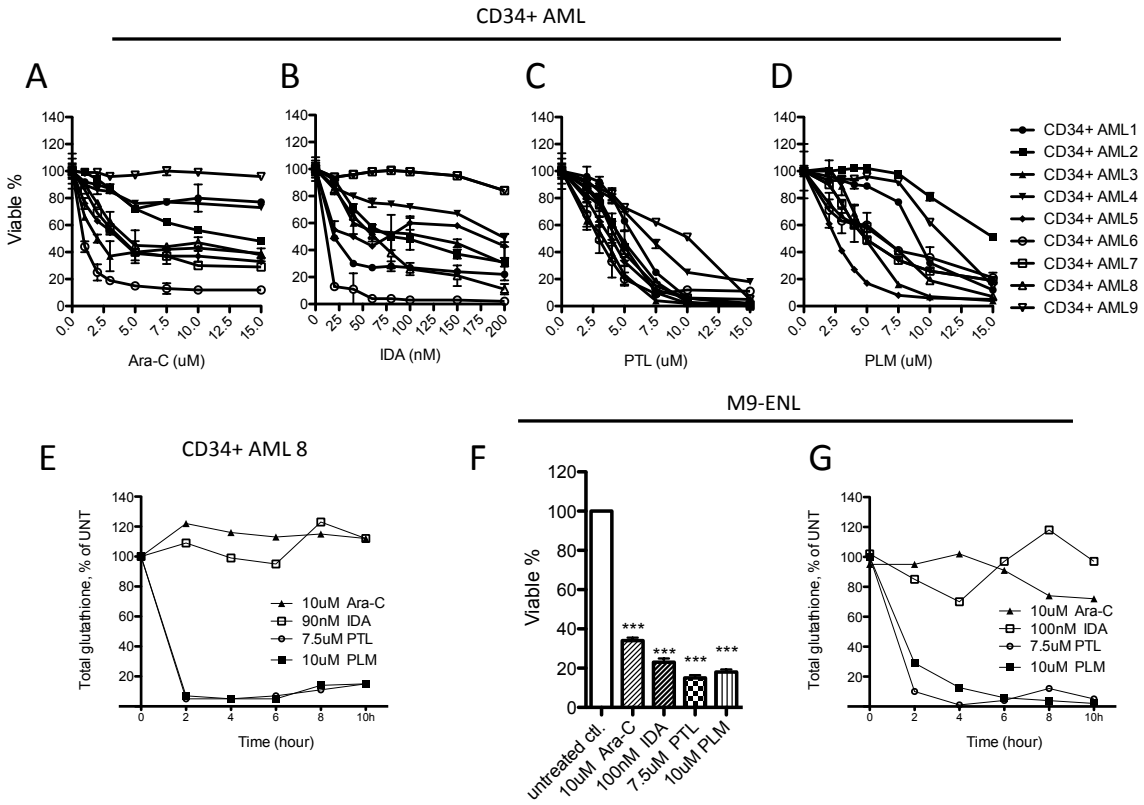

Figure 6

Parthenolide and Piperlongumine represent a novel class of anti-leukemic agents.

Viability of CD34+ AML cells (n=9) treated 24 hours with increasing doses of Ara-C (**A**), IDA (**B**), PTL (**C**) or PLM (**D**). **(E)** Representative graph showing cellular glutathione level change over time in CD34+ AML cells treated with Ara-C, IDA, PTL or PLM. **(F)** Viability of M9-ENL cells treated 24 hours with Ara-C, IDA, PTL or PLM at indicated doses. **(G)** Cellular glutathione level change over time in M9-ENL cells treated with Ara-C, IDA, PTL or PLM. In A, B, C, D and F, mean ± SD of triplicates is presented for each data point. In F, ***p<0.0005.

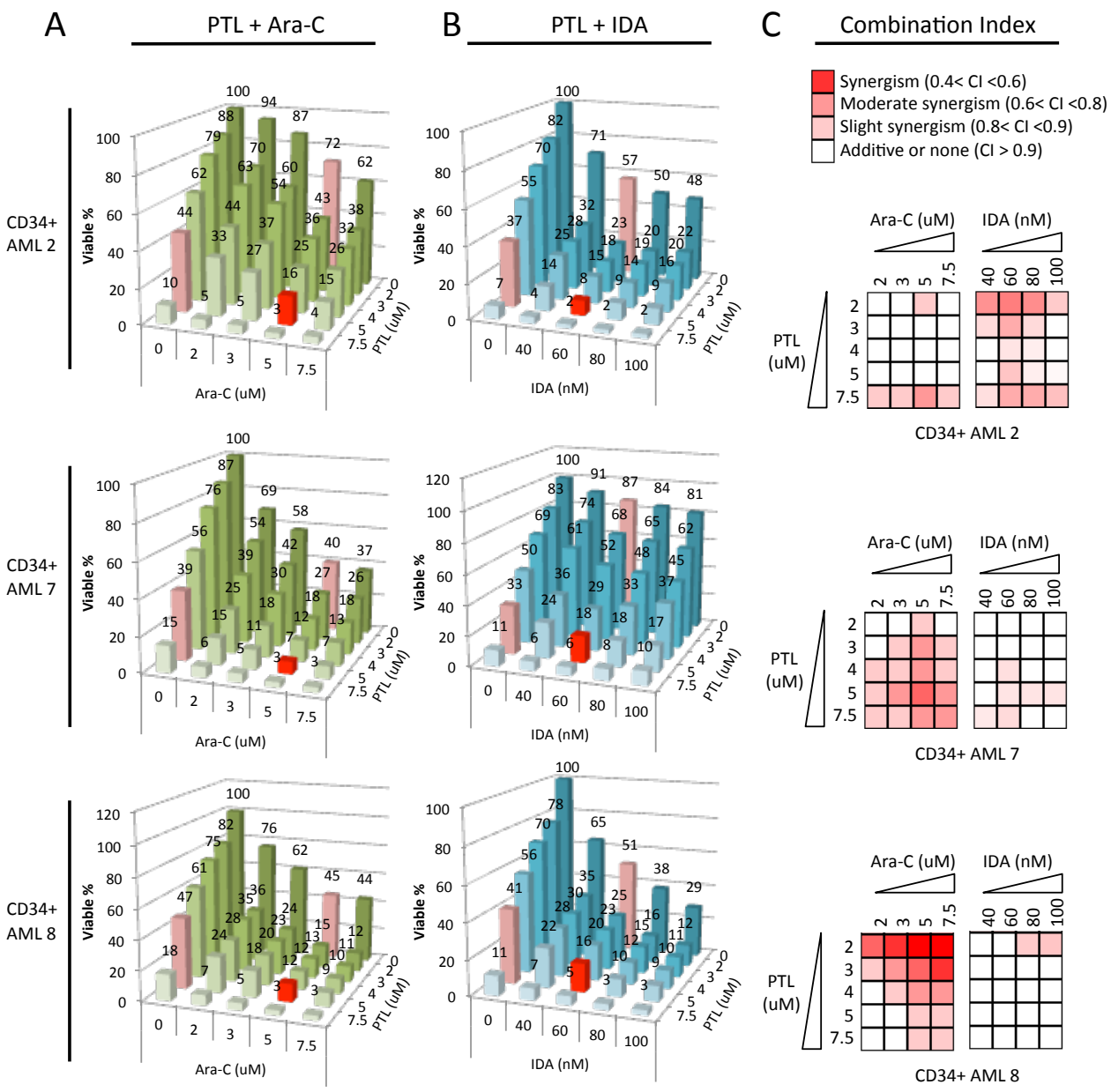

Figure 7

Toxicity of PTL in combination with conventional anti-leukemic agents.

Viability of CD34+ AML cells treated with PTL + Ara-C (**A**) or PTL + IDA (**B**) at various dose combinations. Mean of triplicates is presented. Numbers indicate mean viability. In A, viability of cells treated with 5uM PTL alone, 5uM Ara-C alone, and 5uM PTL + 5uM Ara-C combination are highlighted as red bars. In B, viability of cells treated with 5uM PTL alone, 60nM IDA alone, and 5uM PTL + 60nM IDA combination are highlighted as red bars as well. (**C**) Heat map showing the degree of synergy for each drug combination at fixed dose combo in each AML specimen. Synergism is determined by the combination index (CI) calculated by Calcusyn software. Color key for each category is presented at the top of graph: synergism (0.4 < CI < 0.6), moderate synergism (0.6 < CI < 0.8), slight synergism (0.8 < CI < 0.9), additive or none (CI > 0.9).

Key Research Accomplishments

We have performed a detailed analysis of parthenolide mechanism in leukemia cells.

Reportable outcomes

Manuscript submitted

Conclusion

The differentially response of normal vs. leukemia cells with regard to glutathione metabolism may explain the leukemia-specific activity of parthenolide.

References

1. Couzin, J. 2002. Cancer drugs. Smart weapons prove tough to design. *Science* 298:522-525.
2. Gerlinger, M., Rowan, A.J., Horswell, S., Larkin, J., Endesfelder, D., Gronroos, E., Martinez, P., Matthews, N., Stewart, A., Tarpey, P., et al. 2012. Intratumor heterogeneity and branched evolution revealed by multiregion sequencing. *N Engl J Med* 366:883-892.
3. Patel, J.P., Gonen, M., Figueroa, M.E., Fernandez, H., Sun, Z., Racevskis, J., Van Vlierberghe, P., Dolgalev, I., Thomas, S., Aminova, O., et al. 2012. Prognostic relevance of integrated genetic profiling in acute myeloid leukemia. *N Engl J Med* 366:1079-1089.
4. Skrtic, M., Sriskanthadevan, S., Jhas, B., Gebbia, M., Wang, X., Wang, Z., Hurren, R., Jitkova, Y., Gronda, M., Maclean, N., et al. 2011. Inhibition of mitochondrial translation as a therapeutic strategy for human acute myeloid leukemia. *Cancer Cell* 20:674-688.
5. Samudio, I., Harmancey, R., Fiegl, M., Kantarjian, H., Konopleva, M., Korchin, B., Kaluarachchi, K., Bornmann, W., Duvvuri, S., Taegtmeyer, H., et al. 2010. Pharmacologic inhibition of fatty acid oxidation sensitizes human leukemia cells to apoptosis induction. *J Clin Invest* 120:142-156.
6. Szatrowski, T.P., and Nathan, C.F. 1991. Production of large amounts of hydrogen peroxide by human tumor cells. *Cancer Res* 51:794-798.
7. Trachootham, D., Zhou, Y., Zhang, H., Demizu, Y., Chen, Z., Pelicano, H., Chiao, P.J., Achanta, G., Arlinghaus, R.B., Liu, J., et al. 2006. Selective killing of oncogenically transformed cells through a ROS-mediated mechanism by beta-phenylethyl isothiocyanate. *Cancer Cell* 10:241-252.
8. Hole, P.S., Darley, R.L., and Tonks, A. 2011. Do reactive oxygen species play a role in myeloid leukemias? *Blood* 117:5816-5826.
9. Conklin, K.A. 2004. Chemotherapy-associated oxidative stress: impact on chemotherapeutic effectiveness. *Integr Cancer Ther* 3:294-300.
10. Griffith, O.W., and Mulcahy, R.T. 1999. The enzymes of glutathione synthesis: gamma-glutamylcysteine synthetase. *Adv Enzymol Relat Areas Mol Biol* 73:209-267, xii.
11. Griffith, O.W. 1999. Biologic and pharmacologic regulation of mammalian glutathione synthesis. *Free Radic Biol Med* 27:922-935.
12. Oppenheimer, L., Wellner, V.P., Griffith, O.W., and Meister, A. 1979. Glutathione synthetase. Purification from rat kidney and mapping of the substrate binding sites. *J Biol Chem* 254:5184-5190.
13. Lu, S.C. 2012. Glutathione synthesis. *Biochim Biophys Acta*.

14. Arner, E.S., and Holmgren, A. 2000. Physiological functions of thioredoxin and thioredoxin reductase. *Eur J Biochem* 267:6102-6109.
15. Schenk, H., Klein, M., Erdbrugger, W., Droge, W., and Schulze-Osthoff, K. 1994. Distinct effects of thioredoxin and antioxidants on the activation of transcription factors NF-kappa B and AP-1. *Proc Natl Acad Sci U S A* 91:1672-1676.
16. Chelikani, P., Fita, I., and Loewen, P.C. 2004. Diversity of structures and properties among catalases. *Cell Mol Life Sci* 61:192-208.
17. Tainer, J.A., Getzoff, E.D., Richardson, J.S., and Richardson, D.C. 1983. Structure and mechanism of copper, zinc superoxide dismutase. *Nature* 306:284-287.
18. Borgstahl, G.E., Parge, H.E., Hickey, M.J., Beyer, W.F., Jr., Hallewell, R.A., and Tainer, J.A. 1992. The structure of human mitochondrial manganese superoxide dismutase reveals a novel tetrameric interface of two 4-helix bundles. *Cell* 71:107-118.
19. Guzman, M.L., Rossi, R.M., Karnischky, L., Li, X., Peterson, D.R., Howard, D.S., and Jordan, C.T. 2005. The sesquiterpene lactone parthenolide induces apoptosis of human acute myelogenous leukemia stem and progenitor cells. *Blood* 105:4163-4169.
20. Costello, R.T., Mallet, F., Gaugler, B., Sainty, D., Arnoulet, C., Gastaut, J.A., and Olive, D. 2000. Human acute myeloid leukemia CD34+/CD38- progenitor cells have decreased sensitivity to chemotherapy and Fas-induced apoptosis, reduced immunogenicity, and impaired dendritic cell transformation capacities. *Cancer Res* 60:4403-4411.
21. Ishikawa, F., Yoshida, S., Saito, Y., Hijikata, A., Kitamura, H., Tanaka, S., Nakamura, R., Tanaka, T., Tomiyama, H., Saito, N., et al. 2007. Chemotherapy-resistant human AML stem cells home to and engraft within the bone-marrow endosteal region. *Nat Biotechnol* 25:1315-1321.
22. Guzman, M.L., Neering, S.J., Upchurch, D., Grimes, B., Howard, D.S., Rizzieri, D.A., Luger, S.M., and Jordan, C.T. 2001. Nuclear factor-kappaB is constitutively activated in primitive human acute myelogenous leukemia cells. *Blood* 98:2301-2307.
23. Krause, D.S., Fackler, M.J., Civin, C.I., and May, W.S. 1996. CD34: structure, biology, and clinical utility. *Blood* 87:1-13.
24. Valente, V., Teixeira, S.A., Neder, L., Okamoto, O.K., Oba-Shinjo, S.M., Marie, S.K., Scrideli, C.A., Paco-Larson, M.L., and Carlotti, C.G., Jr. 2009. Selection of suitable housekeeping genes for expression analysis in glioblastoma using quantitative RT-PCR. *BMC Mol Biol* 10:17.
25. de Kok, J.B., Roelofs, R.W., Giesendorf, B.A., Pennings, J.L., Waas, E.T., Feuth, T., Swinkels, D.W., and Span, P.N. 2005. Normalization of gene expression measurements in tumor tissues: comparison of 13 endogenous control genes. *Lab Invest* 85:154-159.
26. Sauerbrey, A., Zintl, F., and Volm, M. 1994. P-glycoprotein and glutathione S-transferase pi in childhood acute lymphoblastic leukaemia. *Br J Cancer* 70:1144-1149.
27. Schisselbauer, J.C., Silber, R., Papadopoulos, E., Abrams, K., LaCreta, F.P., and Tew, K.D. 1990. Characterization of glutathione S-transferase expression in lymphocytes from chronic lymphocytic leukemia patients. *Cancer Res* 50:3562-3568.
28. Friesen, C., Kiess, Y., and Debatin, K.M. 2004. A critical role of glutathione in determining apoptosis sensitivity and resistance in leukemia cells. *Cell Death Differ* 11 Suppl 1:S73-85.
29. Franco, R., and Cidlowski, J.A. 2009. Apoptosis and glutathione: beyond an antioxidant. *Cell Death Differ* 16:1303-1314.
30. Armstrong, J.S., Steinauer, K.K., Hornung, B., Irish, J.M., Lecane, P., Birrell, G.W., Peehl, D.M., and Knox, S.J. 2002. Role of glutathione depletion and reactive oxygen species generation in apoptotic signaling in a human B lymphoma cell line. *Cell Death Differ* 9:252-263.
31. Adams, D.J., Dai, M., Pellegrino, G., Wagner, B.K., Stern, A.M., Shamji, A.F., and Schreiber, S.L. 2012. Synthesis, cellular evaluation, and mechanism of action of piperlongumine analogs. *Proc Natl Acad Sci U S A*.
32. Raj, L., Ide, T., Gurkar, A.U., Foley, M., Schenone, M., Li, X., Tolliday, N.J., Golub, T.R., Carr, S.A., Shamji, A.F., et al. 2011. Selective killing of cancer cells by a small molecule targeting the stress response to ROS. *Nature* 475:231-234.
33. Mullenbach, G.T., Tabrizi, A., Irvine, B.D., Bell, G.I., and Hallewell, R.A. 1987. Sequence of a cDNA coding for human glutathione peroxidase confirms TGA encodes active site selenocysteine. *Nucleic Acids Res* 15:5484.
34. Hamilton, D., Wu, J.H., Alaoui-Jamali, M., and Batist, G. 2003. A novel missense mutation in the gamma-glutamylcysteine synthetase catalytic subunit gene causes both decreased enzymatic activity and glutathione production. *Blood* 102:725-730.

35. Tu, Z., and Anders, M.W. 1998. Identification of an important cysteine residue in human glutamate-cysteine ligase catalytic subunit by site-directed mutagenesis. *Biochem J* 336 (Pt 3):675-680.
36. Fraser, J.A., Kansagra, P., Kotecki, C., Saunders, R.D., and McLellan, L.I. 2003. The modifier subunit of Drosophila glutamate-cysteine ligase regulates catalytic activity by covalent and noncovalent interactions and influences glutathione homeostasis in vivo. *J Biol Chem* 278:46369-46377.
37. Sheehan, D., Meade, G., Foley, V.M., and Dowd, C.A. 2001. Structure, function and evolution of glutathione transferases: implications for classification of non-mammalian members of an ancient enzyme superfamily. *Biochem J* 360:1-16.
38. Franklin, C.C., Backos, D.S., Mohar, I., White, C.C., Forman, H.J., and Kavanagh, T.J. 2009. Structure, function, and post-translational regulation of the catalytic and modifier subunits of glutamate cysteine ligase. *Mol Aspects Med* 30:86-98.
39. Nasim, S., Pei, S., Hagen, F.K., Jordan, C.T., and Crooks, P.A. 2010. Melampomagnolide B: a new antileukemic sesquiterpene. *Bioorg Med Chem* 19:1515-1519.
40. Kwok, B.H., Koh, B., Ndubuisi, M.I., Elofsson, M., and Crews, C.M. 2001. The anti-inflammatory natural product parthenolide from the medicinal herb Feverfew directly binds to and inhibits IkappaB kinase. *Chem Biol* 8:759-766.
41. Asahi, M., Fujii, J., Takao, T., Kuzuya, T., Hori, M., Shimonishi, Y., and Taniguchi, N. 1997. The oxidation of selenocysteine is involved in the inactivation of glutathione peroxidase by nitric oxide donor. *J Biol Chem* 272:19152-19157.
42. Barabe, F., Kennedy, J.A., Hope, K.J., and Dick, J.E. 2007. Modeling the initiation and progression of human acute leukemia in mice. *Science* 316:600-604.
43. Rushworth, S.A., Bowles, K.M., and MacEwan, D.J. 2011. High basal nuclear levels of Nrf2 in acute myeloid leukemia reduces sensitivity to proteasome inhibitors. *Cancer Res* 71:1999-2009.
44. Yang, H., Magilnick, N., Lee, C., Kalmaz, D., Ou, X., Chan, J.Y., and Lu, S.C. 2005. Nrf1 and Nrf2 regulate rat glutamate-cysteine ligase catalytic subunit transcription indirectly via NF-kappaB and AP-1. *Mol Cell Biol* 25:5933-5946.
45. Xia, C., Hu, J., Ketterer, B., and Taylor, J.B. 1996. The organization of the human GSTP1-1 gene promoter and its response to retinoic acid and cellular redox status. *Biochem J* 313 (Pt 1):155-161.
46. Trachootham, D., Zhang, H., Zhang, W., Feng, L., Du, M., Zhou, Y., Chen, Z., Pelicano, H., Plunkett, W., Wierda, W.G., et al. 2008. Effective elimination of fludarabine-resistant CLL cells by PEITC through a redox-mediated mechanism. *Blood* 112:1912-1922.
47. Fernandez-Checa, J.C., Kaplowitz, N., Garcia-Ruiz, C., Colell, A., Miranda, M., Mari, M., Ardite, E., and Morales, A. 1997. GSH transport in mitochondria: defense against TNF-induced oxidative stress and alcohol-induced defect. *Am J Physiol* 273:G7-17.
48. Forman, H.J., Zhang, H., and Rinna, A. 2009. Glutathione: overview of its protective roles, measurement, and biosynthesis. *Mol Aspects Med* 30:1-12.
49. Er, T.K., Tsai, S.M., Wu, S.H., Chiang, W., Lin, H.C., Lin, S.F., Tsai, L.Y., and Liu, T.Z. 2007. Antioxidant status and superoxide anion radical generation in acute myeloid leukemia. *Clin Biochem* 40:1015-1019.
50. Battisti, V., Maders, L.D., Bagatini, M.D., Santos, K.F., Spanevello, R.M., Maldonado, P.A., Brule, A.O., Araujo Mdo, C., Schetinger, M.R., and Morsch, V.M. 2008. Measurement of oxidative stress and antioxidant status in acute lymphoblastic leukemia patients. *Clin Biochem* 41:511-518.
51. Sallmyr, A., Fan, J., and Rassool, F.V. 2008. Genomic instability in myeloid malignancies: increased reactive oxygen species (ROS), DNA double strand breaks (DSBs) and error-prone repair. *Cancer Lett* 270:1-9.
52. Sallmyr, A., Fan, J., Datta, K., Kim, K.T., Grosu, D., Shapiro, P., Small, D., and Rassool, F. 2008. Internal tandem duplication of FLT3 (FLT3/ITD) induces increased ROS production, DNA damage, and misrepair: implications for poor prognosis in AML. *Blood* 111:3173-3182.
53. Sattler, M., Verma, S., Shrikhande, G., Byrne, C.H., Pride, Y.B., Winkler, T., Greenfield, E.A., Salgia, R., and Griffin, J.D. 2000. The BCR/ABL tyrosine kinase induces production of reactive oxygen species in hematopoietic cells. *J Biol Chem* 275:24273-24278.
54. Hedley, D.W., McCulloch, E.A., Minden, M.D., Chow, S., and Curtis, J. 1998. Antileukemic action of buthionine sulfoximine: evidence for an intrinsic death mechanism based on oxidative stress. *Leukemia* 12:1545-1552.
55. Hassane, D.C., Guzman, M.L., Corbett, C., Li, X., Abboud, R., Young, F., Liesveld, J.L., Carroll, M., and Jordan, C.T. 2008. Discovery of agents that eradicate leukemia stem cells using an in silico screen of public gene expression data. *Blood* 111:5654-5662.

56. Weiwer, M., Bittker, J.A., Lewis, T.A., Shimada, K., Yang, W.S., MacPherson, L., Dandapani, S., Palmer, M., Stockwell, B.R., Schreiber, S.L., et al. 2012. Development of small-molecule probes that selectively kill cells induced to express mutant RAS. *Bioorg Med Chem Lett* 22:1822-1826.
57. Akerboom, T.P., and Sies, H. 1981. Assay of glutathione, glutathione disulfide, and glutathione mixed disulfides in biological samples. *Methods Enzymol* 77:373-382.
58. Munger, J., Bennett, B.D., Parikh, A., Feng, X.J., McArdle, J., Rabitz, H.A., Shenk, T., and Rabinowitz, J.D. 2008. Systems-level metabolic flux profiling identifies fatty acid synthesis as a target for antiviral therapy. *Nat Biotechnol* 26:1179-1186.
59. Sali, A., and Blundell, T.L. 1993. Comparative protein modelling by satisfaction of spatial restraints. *J Mol Biol* 234:779-815.
60. Jeudy, S., Monchois, V., Maza, C., Claverie, J.M., and Abergel, C. 2006. Crystal structure of Escherichia coli DkgA, a broad-specificity aldo-keto reductase. *Proteins* 62:302-307.
61. Kratzer, R., Kavanagh, K.L., Wilson, D.K., and Nidetzky, B. 2004. Studies of the enzymic mechanism of Candida tenuis xylose reductase (AKR 2B5): X-ray structure and catalytic reaction profile for the H113A mutant. *Biochemistry* 43:4944-4954.
62. Kozakov, D., Hall, D.R., Beglov, D., Brenke, R., Comeau, S.R., Shen, Y., Li, K., Zheng, J., Vakili, P., Paschalidis, I., et al. 2010. Achieving reliability and high accuracy in automated protein docking: ClusPro, PIPER, SDU, and stability analysis in CAPRI rounds 13-19. *Proteins* 78:3124-3130.
63. Ashton, J.M., Balys, M., Neering, S.J., Hassane, D.C., Cowley, G., Root, D.E., Miller, P.G., Ebert, B.L., McMurray, H.R., Land, H., et al. 2012. Gene sets identified with oncogene cooperativity analysis regulate in vivo growth and survival of leukemia stem cells. *Cell Stem Cell* 11:359-372.
64. Chou, T.-C., and Talalay, P. 1983. Analysis of combined drug effects: a new look at a very old problem. *Trends Pharmacol Sci* 4:450-454.

Appendices

N/A

Project 2

The primary goal of this project is to investigate how standard therapies effect normal CNS stem cells and to develop less toxic regimens for the treatment of cancer:

SOW task #1: To determine whether parthenolide or parthenolide analogs cause CNS damage in animals treated with these substances, and to determine whether parthenolide or parthenolide analogs enhance the damage caused by cytarabine. (Months 1-24)

SOW task #2: Demonstrate that mice in which purified cells are more oxidized in vitro will exhibit more extensive damage from cytarabine, parthenolide (or parthenolide analogs) or the combination of these agents, than those in which purified cells are intrinsically more reduced (Months 25-48).

SOW task #3: To initiate identification of potential prognostic indicators to detect individuals at greater risk for adverse side effects of therapy with cytarabine, parthenolide (or parthenolide analogs) or the combination of these agents, and begin testing to provide proof of principle for protective strategies that involve administration of N-acetyl-L-cysteine (alone or in combination with Vitamins E and/or C) as an anti-oxidant to protect against oxidative damage (Months 49-60).

The safety of parthenolide derivatives

This portion of the research integrates concerns of CNS toxicity of cancer therapies with studies on redox status as an indicator of vulnerability.

In previous project reports, we have provided detailed data for our new studies on toxicity. In brief, we found that most cancer treatment regimens that we examine are toxic for progenitor cells and oligodendrocytes of the CNS. At this stage, we have demonstrated toxicity (both in vitro and in vivo) for BCNU, cisplatin, cyclophasphamide, vincristine, cytarabine, 5-fluorouracil and tamoxifen. We also have examined multiple regions of the CNS. We also found substantial toxicity of parthenolide for CNS progenitor cells.

In our last report we noted that we thought that this portion of the work was essentially completed, but our continued investigations on this topic has led to us the finding that there are some toxicities in vitro that we don't see in vivo. Our current hypothesis is that this is due to blood-brain barrier permeability of the compounds we are using, with compounds that have less permeability being less injurious to the CNS.

Our current hypothesis that is that compounds with low lipophilicity may offer advantages in treating non-CNS cancers, and parthenolide – and more importantly the DMAPT derivative of parthenolide that has already entered clinical trials - is an excellent agent with which to test this possibility.

Examination of the effects of DMAPT on exceptionally vulnerable mice demonstrates that this agent is an outstanding candidate for safe treatment of hematopoietic tumors in respect to concerns about damage to the central nervous system. To conduct these experiments, we examined the effects of DMAPT on mice that have a germline mutation that makes them exceptionally vulnerable to standard cancer treatments. We conducted the experiments in this manner as usage of any therapeutic compound means exposure in people with widely different sensitivities to cancer treatment. Thus, we are concerned to test vulnerability to this compound in conditions in which vulnerability is particularly high.

These experiments were conducted using mice with a germline mutation in the ATM gene. Such mice represent an animal model for the disease ataxia-telangiectasia (A-T). Approximately 30% of children with A-T develop cancer, and most of these cancers are tumors of the hematopoietic system. Treatment of these cancers is extremely challenging as ATM mutations make cells more vulnerable to any agent that causes DNA damage, including oxidative stress.

We found that DMAPT does not increase cell death even in the brains of $ATM^{mut/mut}$ mice**.** In these experiments, we treated $ATM^{mut/mut}$ mice with DMAPT (100mg/kg twice daily, IP, 7 days of treatment) and or with vehicle control. 12 hrs after the last treatment, animals were sacrificed and perfused and analyzed by TUNEL staining to examine apoptosis in the CNS. Twelve 15 μm sections were analyzed from each brain.

Despite the pro-oxidant activity of DMAPT, there was no effect of this agent on cell death in the $ATM^{mut/mut}$ mice. The brains of control mice contained an average of 4.8 TUNEL+ cells per section, while the brains of mice treated with DMAPT contained an average of 3.6 TUNEL+ cells per section. While this work is still ongoing, with additional examination of cell division in the brains of treated animals, results thus far provide a clear indication that treatment of ATM $^{mut/mut}$ mice with an experimentally relevant dosage of DMAPT does not cause increased cell death in the CNS.

Our findings that DMAPT are severely toxic for leukemia TICs but have little or no effect on normal hematopoietic stem cells (HSCs), combined with our present results suggest that this agent is an exceptionally promising candidate to develop as potentially safe new therapeutic agent.

Developing safer approaches to treatment of cancer

The second central concern of this project has been to develop safer treatments or by developing novel means of protecting normal cells from the toxic effects of existing chemotherapeutic agents.

In work leading up to this report, we found that it was possible to protect against many aspects of chemotherapy-mediated damage with erythropoietin (EPO). This exciting possibility was the focus of last year's report because of its potential for clinical relevance as well as for its importance to how we approach the problem of understanding the underlying mechanisms

We have been trying to understand the mechanism of action of EPO, and this has tied in with our work on anti-oxidants due to findings that EPO can stimulate activity of Nrf2, a key regulator of the anti-oxidant element promoter that controls phase 2 detoxifying enzymes and is thus a key regulator of redox status.

At the same time as conducting this work, it has become increasingly clear that the use of EPO as a component of cancer treatment is very problematic, as EPO appears to be able to provide protection to cancer cells that express EPO receptors.

In addition, the studies in Task 1 and Task 2 have indicated that although there may be opportunities to utilize redox regulation as a means of treating cancer, it is necessary to identify mechanisms that distinguish between the utilization of redox status in cancer cells and in normal cells. Thus, in parallel with the studies on Task 1 we have pursued parallel analyses on how we might harness such differences to develop safer cancer treatments.

Of particular promise in this regard is that we have been repurposing the use of tamoxifen (TMX) to treat a variety of cancers through estrogen receptor α (ERα)-independent mechanisms. We have discovered, in other parts of our overall research program, that the ability of the known pro-oxidant activities of TMX to induce cancer cell death is inhibited due to the prevention of activation of the c-Cbl ubiquitin ligase. In primary cells, TMX activates c-Cbl as a consequence of oxidation-mediated activation of Fyn kinase, which in turn phosphorylates and activates c-Cbl. Overexpression of Cdc42 disrupts Fyn-mediated activation of c-Cbl.

The above discoveries led us to the discovery that a Cdc42-specific inhibitor (called ML141) can enhance the sensitivity of multiple different tumor types to TMX. This is of great potential interest, as use of high-dose TMX has been pursued for over a dozen different cancers (including cancers of the hematopoietic system), but there have been virtually no studies on how to enhance the utility of the ERα-independent activities of TMX.

Based on our very promising results with basal-like breast cancers, we extended our work on ML141 and TMX to analysis of T-cell lymphomas isolated from $ATM^{mut/mut}$ mice. These tumors were of particular interest due to the increasing recognition of the importance ATM mutations in tumors of the hematopoietic system. While ML141 by itself was not effective on these cells, the combination of 10 μM ML141 + 10 μM TMX completely eliminated all $ATM^{mut/mut}$ cells. This is a level of sensitivity that even exceeds that seen in our parallel work on enhancing sensitivity to TMX in basal-like breast cancer cells and oesophageal cancer cells.

Moreover, when we compared the efficacy of TMX + ML141 on elimination of $ATM^{mut/mut}$ T-cell lymphomas, we found that the combination of TMX+ ML141 was considerably more effective.

We next analyzed whether ML141 enhances the sensitivity of normal brain cells to TMX. As for DMAPT, results were very promising in that although ML141 enhanced vulnerability to TMX in multiple different cancer cells it did not enhance the vulnerability of normal CNS cells to this agent.

Key Research Accomplishments

We have demonstrated that even in a strain of mice that is exceptionally vulnerable to physiological stressors, including those important in cancer treatment, the parthenolide derivative DMAPT does not cause apparent damage to the CNS. Thus, this highly effective agent appears to be a particularly safe candidate for further examination.

Through analysis of different ways in which normal cells and cancer cells respond to redox changes, we also have identified a second strategy by which we can harness estrogen-receptor-independent pro-oxidative activities of TMX to more effectively kill a variety of cancer cells. In analysis of T-cell lymphomas from mice with mutations in the ATM gene we found that this new strategy (which combines the Cdc42 inhibitor ML141 with TMX) is even more effective at killing these cells than DMAPT.

Conclusion

The use of DMAPT as a potential cancer treatment agent offers an unusual safety profile that appears to spare the CNS from damage. In addition, the information obtained from studies on parthenolide-related redox biology and TMX-related redox biology has revealed a second strategy for harnessing directed targeting of redox status in a manner that appears to be suitable for treating cancer in safter and more effective manners.

Thus, the research supported by this funding has placed us on very firm ground for the development of better cancer therapies and, more importantly, has provided insights likely to prove of a much more general applicability in achieving this important goal.

Reportable outcomes

Pending

Appendices

N/A